Filter-Based Active Damping of Voltage Source Converters With LCL Filter

Joerg Dannehl, *Member, IEEE*, Marco Liserre, *Senior Member, IEEE*, and Friedrich Wilhelm Fuchs, *Senior Member, IEEE*

***Abstract*—Pulsewidth modulation (PWM) voltage source converters are becoming a popular interface to the power grid for many applications. Hence, issues related to the reduction of PWM harmonics injection in the power grid are becoming more relevant. The use of high-order filters like LCL filters is a standard solution to provide the proper attenuation of PWM carrier and sideband voltage harmonics. However, those grid filters introduce potentially unstable dynamics that should be properly damped either passively or actively. The second solution suffers from control and system complexity (a high number of sensors and a high-order controller), even if it is more attractive due to the absence of losses in the damping resistors and due to its flexibility. An interesting and straightforward active damping solution consists in plugging in, in cascade to the main controller, a filter that should damp the unstable dynamics. No more sensors are needed, but there are open issues such as preserving the bandwidth, robustness, and limited complexity. This paper provides a systematic approach to the design of filter-based active damping methods. The tuning procedures, performance, robustness, and limitations of the different solutions are discussed with theoretical analysis, selected simulation, and experimental results.**

***Index Terms*—Active resonance damping, current control, grid-connected pulsewidth modulation (PWM) converters, LCL filters.**

I. Introduction

PULSEWIDTH MODULATION (PWM) voltage source converters (VSCs) are increasingly used to connect different players to the bulky power system: electric drives, distributed power generation systems, loads, power quality conditioners, energy storage systems, flexible ac transmission, and high-voltage dc transmission systems [1]–[3]. No matter if the power converter exchanges active or reactive power, fundamental component or harmonics, direct sequence and/or inverse sequence, a filter is needed to get rid of the PWM carrier and sideband harmonics [4]–[6]. Typically, the filter is a high-order low-pass filter such as the LCL filter. More complex filters may be adopted, but they should exhibit low-frequency first-order (inductive) behavior to allow for proper active/reactive power control and exhibit high-frequency low-pass behavior to guarantee proper filtering even of the higher order harmonics that are typically constrained by more stringent limitations. The dynamics associated to the low-frequency range are usually controlled by a current control loop while the dynamics associated to the high-frequency range (resonant poles that guarantee a 60-dB/dec attenuation of the PWM voltage harmonics) are damped by modifying the filter structure with the addition of passive elements or by acting on the parameters or on the structure of the controller. The first option is referred to as passive damping while the second is referred to as active damping. Both need to be robust with respect to the parameter variation [7]–[9]. Passive damping causes a decrease of the overall system efficiency because of the losses associated that are partly caused by the low-frequency harmonics (fundamental and undesired pollution) present in the state variables and partly by the switching frequency harmonics [4]. Moreover, passive damping reduces the filter effectiveness since it is very difficult to insert the damping in a selective way at those frequencies where the system is resonating due to a lack of impedance. As a consequence, the passive damping is always present, and the filter attenuation at the switching frequency is compromised [4]. Selective passive damping solutions are also possible and interesting for high-power systems [10]. Active damping consists in modifying the controller parameters or the controller structure increasing the magnitude and phase margins around the resonance frequency [11]–[13]. Active damping methods are more selective in their action; they do not produce losses, but they are also more sensitive to parameter uncertainties [7], [14]. Moreover, the possibility to control the potential unstable dynamics is limited by the controller sampling frequency that should be at least double with respect to the resonance frequency to perform the active damping [11], [12], [15].

The aim of this paper is to review the active damping methods based on the use of digital filters, in a systematic way. Different resonance frequencies and different sensor positions are taken into account in the analysis. Tuning and implementation issues are considered, and the proposed methods are compared also in view of their influence on the controller bandwidth and of their robustness to parameter uncertainty. In order to highlight the active damping mechanism on the basis of which these methods work, three classes of second-order filters are

Manuscript received December 23, 2009; revised April 20, 2010 and July 28, 2010; accepted September 6, 2010. Date of publication September 30, 2010; date of current version July 13, 2011. This work was supported by the German Research Foundation (DFG).

J. Dannehl was with the Institute for Power Electronics and Electrical Drives, Christian-Albrechts-University of Kiel, 24143 Kiel, Germany. He is now with Danfoss Solar Inverters A/S, 6400 Sønderborg, Denmark (e-mail: dannehl@ieee.org).

M. Liserre is with the Department of Electrical and Electronic Engineering, Politecnico di Bari, 70125 Bari, Italy (e-mail: liserre@ieee.org).

F. W. Fuchs is with the Institute for Power Electronics and Electrical Drives, Christian-Albrechts-University of Kiel, 24143 Kiel, Germany (e-mail: fwf@tf.uni-kiel.de).

Color versions of one or more of the figures in this paper are available online at http://ieeexplore.ieee.org.

Digital Object Identifier 10.1109/TIE.2010.2081952

discussed and proven experimentally: low-pass, lead-lag, and notch filters. Their combination can be used to design higher order filters for active damping, when needed.

In Section II, the main active damping methods are presented in a critical way. In Section III, the system model is presented, considering also the different sensor positions, and the parameters are given in order to create different resonance scenarios. In Section IV, the stability is analyzed without damping to point out the demands for active damping algorithms. In Section V, different active damping solutions based on the filtering approach are theoretically reviewed. In Section VI, the tuning of these solutions is addressed. In Section VII, the robustness of the presented damping solutions is discussed. Finally, in Section VIII, the experimental results are given to prove the analysis carried out in the previous sections.

II. Overview of Active Damping Methods

Active damping methods can be classified into two main classes: multiloop- and filter-based active damping. In the first case, the stability is guaranteed via the control of more system state variables that are measured or estimated [16]–[21]. Hence, instead of a single current control loop, two or even three control loops are adopted, or an interesting alternative is to split the filtering capacitor in two in parallel and use the current flowing among them as a weighted average of the converter-side and grid-side currents [8]. The implementation can be either based on voltage-oriented control [22], [23] or direct power control [24], sometimes exploiting the popular alternative to the phase-locked loop, the virtual flux, to reduce the number of sensors [25], [26]. Among the controlled state variables, the capacitor voltage can also be controlled in view of the stand-alone or microgrid operation using droop control [27]. This approach can be formalized within the more general theoretical framework of the state-space control [28]–[33] also using a state estimator [34], [35], sometimes in combination with predictive control [36], [37]. Further and interesting developments have been carried out analyzing the stability through the convergence of state trajectories to an orbit [38] or through flatness and passivity properties [39], [40].

The second class of active damping methods is based on the use of a higher order controller not only to regulate the low-frequency dynamics but also to damp the high-frequency ones. The controller part responsible for the active damping of the potentially unstable high-frequency dynamics can be seen as a filter [41]. The filter can be designed using different approaches: Two have been proposed in the literature for active damping purposes. The first consists in designing an analog filter, typically a notch filter, and then applying analog-to-discrete transformation based on a given set of specifications, called bilinear transformation [42]. The second approach consists in designing directly the filter in the Z-domain and, hence, in choosing the coefficients of the digital form of the filter, sometimes using advanced optimization tools like genetic algorithms [41], [43]. In both cases, this class of active damping methods has the advantage that it does not need more sensors. However, only in the case of the first approach is the straightforward physical meaning of "filtering" the resonance preserved.

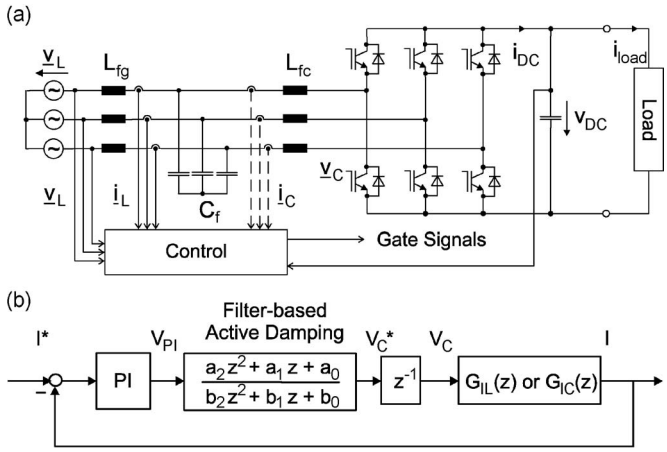

Fig. 1. LCL-filter-based grid-connected VSCs. (a) Hardware and control scheme (where either grid current or converter current is sensed). (b) Current control loop model.

III. System Model

Fig. 1(a) shows the grid-connected VSC with the LCL filter. The converter controller typically consists of an outer dc link voltage controller with an inner active grid current loop [1]. The same current controller is used for controlling the reactive grid current. The current loop is emphasized in this paper. As both the line-current feedback and converter-current feedback are considered in this paper, the following two transfer functions of a lossless LCL filter from the converter output voltage V_C to the ac output current I_L or I_C, respectively, are of interest:

$$G_{IL}(s) = \frac{I_L(s)}{V_C(s)} = \frac{1}{L_{\rm fc}L_{\rm fg}C_f \cdot s}\frac{1}{s^2+\omega_{\rm Res}^2} \tag{1}$$

$$G_{IC}(s) = \frac{I_C(s)}{V_C(s)} = \frac{1}{L_{\rm fc} \cdot s}\frac{s^2+\omega_0^2}{s^2+\omega_{\rm Res}^2} \tag{2}$$

with $\omega_{\rm Res} = 2\pi f_{\rm Res} = \sqrt{(L_{\rm fg}+L_{\rm fc})/(L_{\rm fg}L_{\rm fc}C_f)}$ and $\omega_0 = \sqrt{1/(L_{\rm fc}C_f)}$ being the resonance frequency and antiresonance frequency, respectively. The main difference between (1) and (2) is the zeros in the transfer function of G_{IC} at ω_0. They introduce a negative peak at ω_0 and cause less damping and phase lag at frequencies above $\omega_{\rm Res}$ as they compensate the effect of two poles. The losses, neglected in (1) and (2) for the sake of simplicity, influence the real damping of the system potential unstable dynamics, and they have been correctly identified as discussed in [44].

For the stability and performance analysis, the discrete control loop model of Fig. 1(b) is used. The loop consists of the proportional-plus-integral (PI) controller (backward implementation), the filter for active damping, a one-sample computational delay (T_C) representing the converter, and the LCL transfer function discretized with a zero-order hold. Either (1) or (2) is used, depending on which current is sensed.

The ratio of the LCL-filter resonance frequency $f_{\rm Res}$ to the control/sampling frequency $f_c = 1/T_c$ influences the system stability scenario. In order to cover a typical range of ratios, the switching frequency is kept constant at 2.5 kHz, and different LCL settings are considered in this paper (see Table I). The resonance frequency is given in per unit (p.u.) values, whereas

TABLE I
LCL FILTER RESONANCE FREQUENCIES

C_f [μF]	16	32	80
f_{Res} [kHz]	1.7	1.2	0.76
f_{Res} [p.u.]	0.7	0.5	0.3

the base frequency is the Nyquist frequency, i.e., half the control frequency. In this paper, the different LCL settings differ in the filter capacitance (see Table I). The filter inductances are $L_{\rm fg} = 750$ μH (3.7%) and $L_{\rm fc} = 2$ mH (9.9%). The inductor iron losses have been neglected, and the parasitic series resistances have been measured to $R_{\rm fg} = 50$ mΩ and $R_{\rm fc} = 60$ mΩ. However, the results and design guidelines are generic and can be transferred to other settings easily. The rising and falling edges of the gate signal can be controlled independently. Hence, the control frequency is twice the switching frequency: $f_c = 1/T_c = 5$ kHz.

IV. STABILITY ANALYSIS WITHOUT ACTIVE DAMPING

Before studying the active damping filters, the loop without them is analyzed in order to point out the basic problems. For this purpose, stability analysis is carried out by means of the Bode diagrams of the open current control loop in conjunction with the Nyquist stability criterion.

A. Nyquist Criterion in Open-Loop Bode Diagram

The Nyquist stability criterion tells to count $-180°$ crossings in the open-loop Bode diagram only in the frequency range with gains above 0 dB [45]. The number of positive crossings is denoted by S^+, and the number of negative crossings is denoted by S^-. The difference $S^+ - S^-$ must equal zero in this case as there are no unstable poles in the open loop. A nonzero difference indicates instability.

B. Evaluation for Different LCL-Filter Resonance Frequencies

Fig. 2 shows the open-loop Bode diagrams for line-current feedback (a) and converter-current feedback (b) for different LCL-filter resonance frequencies.

For the line-current feedback, the system is stable for the higher resonance frequencies as there are neither positive nor negative $-180°$ crossings in the critical frequency range. With decreasing $f_{\rm Res}$, the stability gets worse. For the LCL filter with the lowest resonance frequency, there is no positive crossing, but there is a negative crossing in the range where the gain is higher than 0 dB [see Fig. 2(a)]. Hence, the Nyquist stability criterion indicates instability. Even though the LCL setting with medium resonance frequency is stable, its stability margins are rather low (minimal phase margin is 25.4° close to the resonance frequency).

For the converter-current feedback, the system is stable only for very low resonance frequencies. It can be seen from Fig. 2(b) that, for low resonance frequencies, the $-180°$ is crossed only once at a frequency higher than the resonance where the gain is lower than 0 dB. Hence, a stable operation is obtained in that case. However, worse resonance damping is

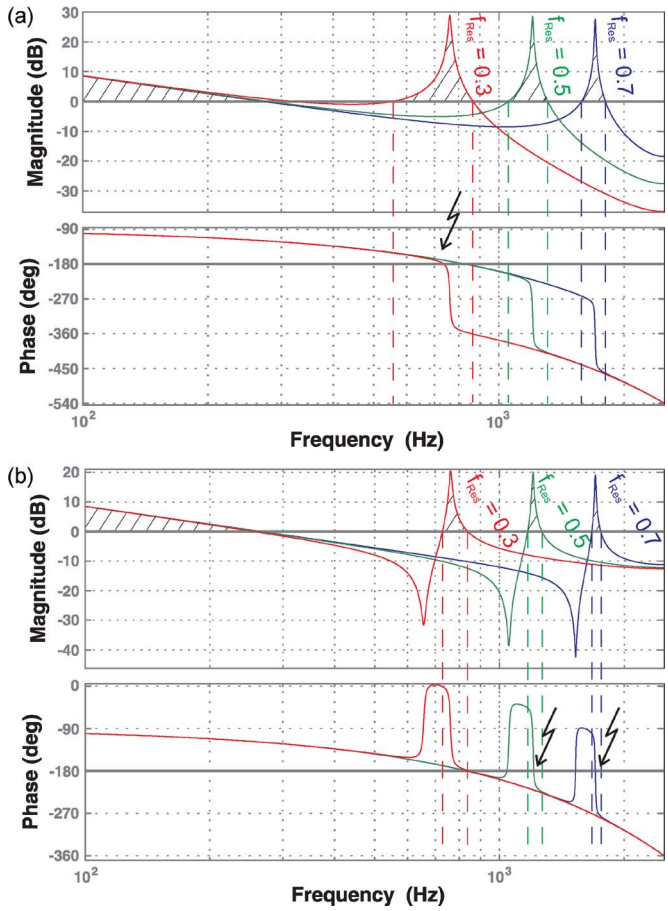

Fig. 2. Open-loop Bode diagram for different LCL-filter resonance frequencies and sensor positions without active damping filters: (a) Line current and (b) converter current. $f_{\rm Res}$ is expressed in p.u. of the base frequency $f_c/2$ (Nyquist frequency).

obtained as the phase margin is very low. In other words, the closed-loop resonance poles remain close to the unity circle. For the higher resonance frequencies, there is one negative $-180°$ crossing and no positive crossings in the relevant frequency range. Thus, the difference of the positive-to-negative crossings is nonzero, and the evaluation of the Nyquist criterion indicates instability. Hence, damping is required for all LCL settings with converter-current feedback.

V. FILTER-BASED ACTIVE DAMPING

In this section, several filters are approached for active damping. The study in this paper is limited to filters with a maximum of two poles and two zeros in order to keep the complexity reasonable. Hence, their generic transfer function can be expressed by

$$G(z) = \frac{a_2 z^2 + a_1 z + a_0}{b_2 z^2 + b_1 z + b_0}. \tag{3}$$

The coefficients a_0, a_1, a_2, b_0, b_1, and b_2 are calculated in the Appendix. Their basic behavior is studied, and the suitability for active damping as part of the current control loop with either line or converter-current feedback is discussed in a qualitative manner. The general demands on the filters are pointed out first.

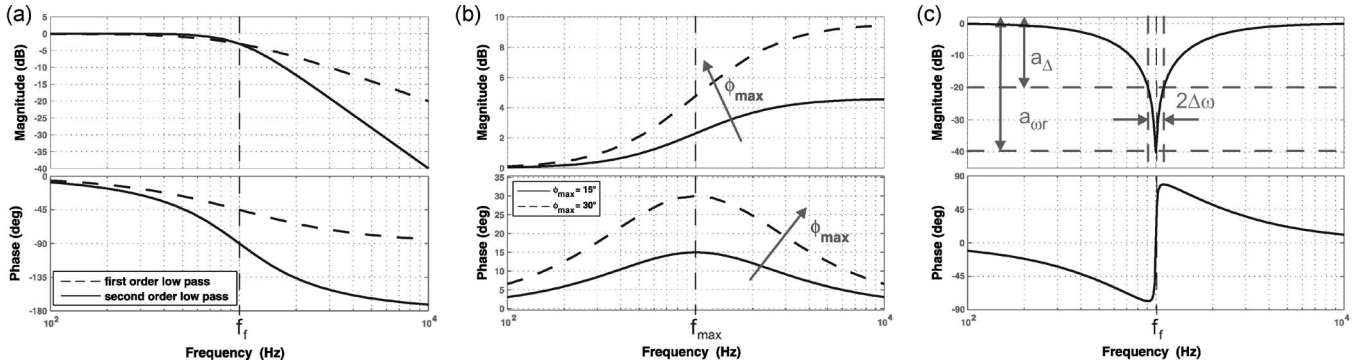

Fig. 3. Characteristic frequency response of different filters. (a) Low-pass filter. (b) Lead element filter. (c) Notch filter ($\omega_f = 2\pi f_f$).

A. Demands on Resonance Damping Filters

Theoretically, it is possible to reduce drastically the proportional gain of the PI controller in order to stabilize the system. However, this yields poor bandwidth and disturbance rejection capability and is not further considered here. The requirement is to obtain resonance damping while preserving reasonable bandwidth as well as stability and robustness margins.

For filter-based active damping, there are basically two possible ways. The first one is to attenuate the resonance peak of the gain response. However, as the resonance peak is very high, a rather sharp filter characteristic is required. Otherwise, the closed-loop bandwidth is decreased considerably. The second way is to avoid -180° crossings in the frequency range with a gain above 0 dB. The resonance frequency range is relevant in that context. Theoretically, a -180° crossing can either be shifted to lower or higher frequencies. It depends on the feedback current and on the resonance frequency whether leading or lagging filters are to be employed. Hence, filters with either leading or lagging behavior can stabilize the system in some cases. However, in some cases, both cannot yield stability. Note that the gain and phase responses cannot be modified separately. The impact of a particular filter on both needs to be studied.

B. Low-Pass Filters

An intuitive choice for filtering is a low-pass filter of the first or second order. The parameters of a second-order low-pass filter are shown in Table VIII in the Appendix. Fig. 3 shows the characteristic frequency response of first-order filters as well as that of second-order filters with $D = 1/\sqrt{2}$. As the gain response is relatively smooth, the resonance peaks in the open-loop gain cannot be eliminated when a reasonable bandwidth is required. Typically, the stability suffers from a phase lag introduced by low-pass filtering. However, for resonance damping, the phase lag can be beneficial in some case, depending on the current sensor position and resonance frequency (see Fig. 2 and [12] and [41]).

For the converter-current feedback with high resonance frequencies, it becomes clear from Fig. 2 that a lagging behavior can stabilize the system as the peak in the phase response at the resonance frequency can be reduced below -180°. The -180° crossing is shifted outside of the frequencies with a gain above 0 dB. However, as the required phase lag increases with decreasing resonance frequency, this filter type is not suitable for lower resonance frequencies.

For the line-current control, the phase lag can be critical for high resonance frequencies as it creates a -180° crossing in the critical frequency range. On the other hand, a phase lag can stabilize the system for low resonance frequencies as the -180° crossing is shifted to lower frequencies where the gain is below zero. A tradeoff between the cutoff frequency and the phase lag is necessary. The cutoff frequency limits the bandwidth in closed-loop operation. When the resonance frequency is close to the desired closed-loop bandwidth, the low-pass filter will give only low resonance damping.

C. Lead-Lag Elements

A lead element introduces a phase lead in a limited frequency band. Its parameters are shown in Table VIII in the Appendix. In dependence of the filter parameters α and ω_f, a phase lead $\phi_{\max}$ is obtained at $\omega_{\max}$. The following relations hold:

$$\sqrt{\alpha} = \tan\left(\frac{\pi}{4} - \frac{\phi_{\max}}{4}\right) \tag{4}$$

$$\omega_f = \omega_{\max}\sqrt{\alpha}. \tag{5}$$

Fig. 3(b) shows the Bode diagram of two lead elements with different phase lead values at the same frequency. It can be seen that the desired phase lead is obtained but the gain at higher frequencies is amplified as well. Hence, the measurement noise will be amplified. This limits the possible phase lead in practice.

For the line-current feedback, this filter type is not suitable because the phase lead is too low. For higher resonance frequencies, it is even worse as it can cause -180° crossings in critical frequency ranges. Anyway, for the converter-current feedback, the system can be stabilized if the required phase lead is not too high. With increasing resonance frequency, the required phase lead increases as well (see Fig. 2). Thus, this filter type is only suitable for lower resonance frequencies. However, the gain margins and the bandwidth are considerably lower compared to that of the other active damping solutions. For this reason, the lead elements are not further considered.

Note that a lag element with a phase lag only around a particular frequency gives no advantage over the low-pass filter. It is not necessary to have a phase lag only around the resonance frequency. Higher frequencies can be damped as well without suffering a closed-loop dynamic.

D. Notch Filter

The notch-filter-based active damping aims at canceling the resonant peak of the Bode diagram of the LCL-filter transfer function (see Fig. 2). The idea is to compensate the LCL resonance peak by an antiresonance peak of the notch filter. Fig. 3(c) shows the Bode diagram of a notch filter. The notch-filter parameters are shown in Table VIII in the Appendix. The deepness and wideness of the notch filter will be decided by the damping of the zeros and of the poles of the filter, D_z and D_p, respectively. The filter attenuation $a_{\omega f}$ at the notch frequency ω_f or deepness, respectively, is tunable as well as the attenuation a_Δ at the border of a specified frequency band $\omega_f \pm \Delta\omega$. The latter determines the filter wideness. In contrast to low-pass filters and lead elements, the notch filter is basically suitable for resonance damping independent of the ratio of the resonance frequency and the control frequency.

VI. Tuning of PI Controller and Active Damping Controller

The design of selected filters for active damping as well as the PI tuning is presented in this section. Proper resonance damping is the basic criterion, but there are other demands that have to be taken into account. In fact, the impacts on the closed-loop bandwidth and the robustness are important issues. The first is related to the tracking performance as well as the disturbance rejection. The robustness against parameter variations is very important as the LCL-filter parameters as well as the grid impedance cannot be known exactly and may also vary during operation. In this paper, all filters must be designed such that LCL-filter parameter variations of up to $\pm 10\%$ can be accepted without destabilizing the closed loop. As the active damping filter changes the open-loop dynamics, the PI gain needs to be adjusted in order to keep the overshoot almost at the same level.

A. Tuning of PI Controller

The PI controllers are tuned considering the overall system dynamics, including active damping. Note that, for simple second-order systems, the phase margin is directly related to the damping factor of the system or overshoot, respectively [46, p. 163]. The system studied in this paper is of a higher order, and depending on the active damping method adopted, several phase margins at different frequencies can occur. Anyway, the dynamic of the dominant closed-loop pole pair, which makes the closed-loop system behave almost like a second-order system, is related to the phase margin of the 0-dB crossing at the lowest frequency, which is referred to as PM_{LF}. In order to avoid current overshoots, the PI gain is tuned such that $PM_{\mathrm{LF}} = 60^\circ$. The PI integrator time constant is calculated by attempting at canceling the effects of the slow time constants of the plant.

B. Low-Pass Filter

The choice of the filter cutoff frequency is a typical tradeoff between the stability margins and the control bandwidth. The closed-loop bandwidth gets reduced more when low resonance frequencies are to be damped. A good tradeoff is obtained when $\omega_f = \omega_{\mathrm{Res}}$ is selected. The damping coefficient is set to $D = 1/\sqrt{2}$. It is worth noting that a simple one-sample delay $G(z) = 1/z$ can also give enough phase lag if the resonance frequency is high enough. The damping effect of the delay has also been demonstrated in [12]. It is not considered in this paper.

C. Notch Filter

For the LCL resonance damping, $\omega_f = \omega_{\mathrm{Res}}$ follows immediately. The notch filter could be tuned to be very frequency selective. However, as LCL-filter elements can vary and, thus, the resonance frequency as well, the notch filter must be tuned to be robust enough. In order to deal with the specified robustness requirement, $\Delta\omega = 0.1\omega_{\mathrm{Res}}$ and $a_\Delta = a_{\mathrm{peak}}$ are selected. The choice of the notch-filter attenuation at the notch frequency itself is a tradeoff between the resonance damping for the nominal case and the amount of control action. A good tradeoff is $a_{\omega f,\mathrm{dB}} = 2a_{\Delta,\mathrm{dB}}$. The filter parameters from Table VIII in the Appendix are obtained as described in the Appendix.

It is worth noting that, in practice, the resonance peak a_{peak} is lower compared with that of Fig. 2 due to iron losses [44], [47]. However, for the a_Δ tuning, the maximum peak value that can be expected should be taken. Hence, it is a rather conservative approach when just copper losses are considered as natural resonance damping.

It is also worth noting that, if the real LCL resonance frequency is estimated, the notch-filter frequency could be adjusted and tuned much more frequency selective. That means that the frequency band $\Delta\omega$ could be reduced to the expected estimation error. The closed-loop dynamic would be increased by that. In fact, ω_{Res} can be estimated by triggering in a controlled way the resonance of the filter [48].

D. Pole-Zero Maps

Fig. 4 shows the effect of active damping filters by means of pole-zero maps for the case with converter-current feedback and a high resonance frequency. It can be seen that the unstable poles are attracted inside the unity circle proofing stability. The low-frequency branches are shifted toward the lower frequencies, indicating a reduced bandwidth. In order to preserve the bandwidth, the position of the zeros and poles should be chosen directly using a different approach. In fact, the antiresonance peak of Fig. 2(b) limits the bandwidth of the closed loop in case of converter-current feedback. The dynamic improvement and resonance damping can be obtained simultaneously in that case by the cancellation of the antiresonant as well as the resonance peak. This cancellation could be done using a filter that exactly matches the inverse of the resonance characteristic of the plant, but the effect of the imperfect cancellation would lead to poor results. An alternative is to use a biquad filter (see Table VIII in the Appendix). The damping coefficients of the zeros and poles are D_z and D_p, respectively, and ω_z and ω_p are their frequencies, respectively. The filter poles and zeros can be placed independently. Typically, ω_z is chosen to be higher than ω_p in order to create the inverse LCL resonance characteristic

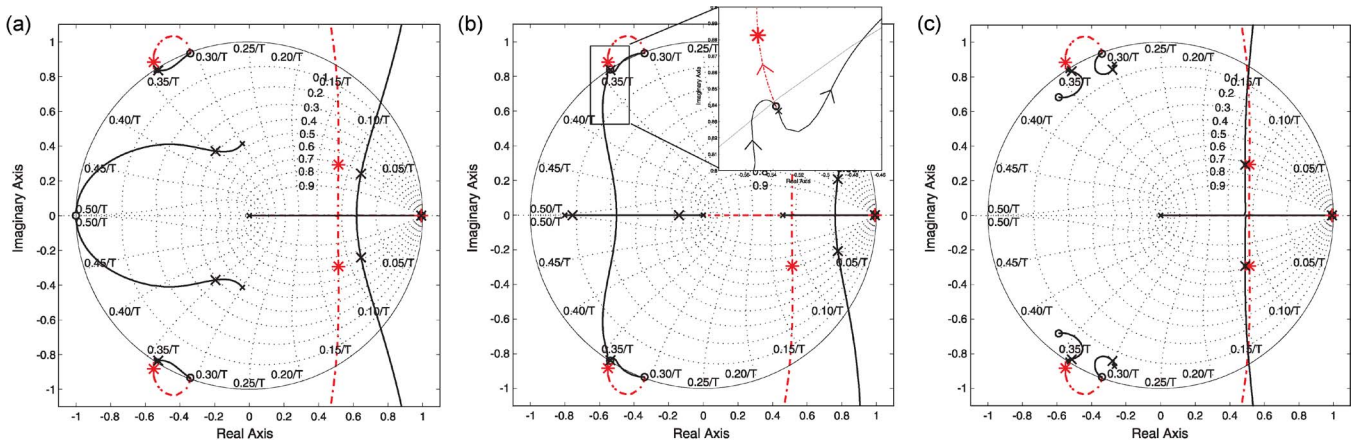

Fig. 4. Pole-zero maps for different active damping filters with converter-current feedback and $f_{\mathrm{Res}} = 0.7 f_c/2$. (a) Low-pass filter. (b) Notch filter. (c) Biquad filter. (Red) No filter. (Black) With filter ($T = 1/f_c$).

TABLE II
NO FILTER WITH CONVERTER-CURRENT FEEDBACK: STABILITY MARGINS AND BANDWIDTH

Resonance Frequency	BW [Hz]	GM_{LF} [dB]	$GM_{HF,min}$ [dB]	$\lvert PM_{HF,min}\rvert$ [°]
high	592	10.2	Unstable (-19)	80
medium	542	12.5	Unstable (-16.9)	45
low	439	0.6	–	1

TABLE III
NO FILTER WITH LINE-CURRENT FEEDBACK: STABILITY MARGINS AND BANDWIDTH

Resonance Frequency	BW [Hz]	GM_{LF} [dB]	$GM_{HF,min}$ [dB]	$\lvert PM_{HF,min}\rvert$ [°]
high	764	8.0	18.5	78
medium	1060	4.7	27.6	25
low	810	Unstable	37.0	29

TABLE IV
LOW-PASS FILTER WITH CONVERTER-CURRENT FEEDBACK: STABILITY MARGINS AND BANDWIDTH

Resonance Frequency	BW [Hz]	GM_{LF} [dB]	$GM_{HF,min}$ [dB]	$\lvert PM_{HF,min}\rvert$ [°
high	404	9.9	–	73.4
medium	346	10.4	Unstable (-4.4)	14
low	268	11.3	Unstable (-10.6)	72

TABLE V
LOW-PASS FILTER WITH LINE-CURRENT FEEDBACK: STABILITY MARGINS AND BANDWIDTH

Resonance Frequency	BW [Hz]	GM_{LF} [dB]	$GM_{HF,min}$ [dB]	$\lvert PM_{HF,min}\rvert$ [°]
high	449	8.4	Unstable (-19.8)	45
medium	424	8.5	17.9	33
low	448	7.4	37.1	91

TABLE VI
NOTCH FILTER WITH CONVERTER-CURRENT FEEDBACK: STABILITY MARGINS AND BANDWIDTH

Resonance Frequency	BW [Hz]	GM_{LF} [dB]	$GM_{HF,min}$ [dB]	$\lvert PM_{HF,min}\rvert$ [°]
high	291	12.0	36.9	–
medium	287	12.4	23.4	–
low	195	15.0	21.6	–

TABLE VII
NOTCH FILTER WITH LINE-CURRENT FEEDBACK: STABILITY MARGINS AND BANDWIDTH

Resonance Frequency	BW [Hz]	GM_{LF} [dB]	$GM_{HF,min}$ [dB]	$\lvert PM_{HF,min}\rvert$ [°]
high	118	17.4	29.8	–
medium	163	14.9	36.6	–
low	99	18	49.6	–

shown in Fig. 2(b). For robustness reasons, the filter frequencies must be tuned such that the LCL resonance poles and zeros lie in between the filter ones for all parameter variation conditions [49]. In Fig. 4(c), the result is shown in order to show the basic principle and difference with respect to the notch-filter approach. The original unstable branches are attracted inside the unity circle. However, the systematic and straightforward filter design procedure for all resonance frequency and current position scenarios, taking into account the robustness requirements, is difficult, and it may need advanced optimization tools [41], [43]. Moreover, there even is no antiresonance that needs to be compensated when the current is sensed at the grid side. For these reasons, this approach is not further studied in detail.

VII. ROBUSTNESS ANALYSIS

The closed-loop performance is studied for the low-pass and notch filters. Moreover, the loop without any damping filters is studied as well. Tables II–VII show the characteristic values. Note that all the filters and PI controllers are tuned in order to obtain a 60° phase margin at the lowest 0-dB crossing. The minimum of all other phase margins is referred to as $PM_{\mathrm{HF,min}}$. The gain margin at the frequency with the first $-180°$ crossing is referred to as GM_{LF}. The minimum of the other gain margins at higher frequencies is $GM_{\mathrm{HF,min}}$. Note that, for some cases, there is only one $-180°$ crossing.

A. No Filter

Tables II and III show the bandwidth and stability margins for the converter-current feedback or line-current feedback, respectively, when no damping filters are in the loop. Only the I_L feedback yields a stable loop with reasonable margins for

LCL filters with high resonance frequency. A low phase margin $|PM_{\mathrm{HF,min}}|$ indicates poor resonance damping and robustness.

B. Low-Pass Filter

Tables IV and V show the bandwidth and stability margins for the converter-current feedback or line-current feedback, respectively, when low-pass damping filters are in the loop. The I_L feedback yields a stable loop with reasonable margins only for LCL filters with low resonance frequency, and the I_C feedback yields a stable loop with reasonable margins only for LCL filters with high resonance frequency.

C. Notch Filter

Tables VI and VII show the bandwidth and stability margins for the converter-current feedback or line-current feedback, respectively, when notch filters are in the loop. Due to the robust design that is required, the bandwidth is low compared to the low-pass filters or "no filtering" option. Moreover, the low-frequency gain margin is also higher, indicating higher robustness to gain variations in the lower frequency range. The minimum gain margin at higher frequencies must be rather high for notch filters as it is rather frequency selective. In case of parameter variations, the open-loop gain diagram changes considerably.

VIII. Results

The active damping performance with notch filters as well as low-pass filters has been experimentally tested on a test drive. This paper provides the results with high and low relative resonance frequencies in order to validate the characteristic differences obtained from the theoretical studies. For this purpose, a fixed filter capacitance of $C_f = 32\ \mu$F and two different control frequencies have been used to obtain different ratios between the control and resonance frequency ($f_C = 4/8$ kHz and $f_{\mathrm{Res}} = 1.2$ kHz). See Section III for the other LCL-filter settings. Tests have been done at a 400-V grid and with a 700-V dc link voltage. The control algorithm is implemented on a dSPACE DS 1006 board. In addition to the PI controller, resonant controllers in parallel are employed for compensating the fifth and seventh harmonics which are caused by background grid voltage distortions. Those are discretized with Tustin approximation and prewarping and are implemented in the dq-frame [50]. The converter supplies a reactive power of 10 kVA (inductive), and no active power is transferred. The robustness of the active damping is verified by simulations with MATLAB/Simulink. The power part, including the insulated-gate bipolar transistors, is modeled with PLECS. The C codes from the experimental tests have been used and embedded into Simulink by S-functions.

A. Test of Effectiveness of Filter-Based Active Damping (Experiments)

In the laboratory, it is possible to run the system stable without active damping filters when the PI controller is tuned with the technical optimum due to the natural passive resonance damping of the LCL filter itself. Poor dynamic performance and robustness margins are obtained in this case. However, it is possible to run the system in a closed loop, and by increasing the PI gain, the excitation of the resonance can be controlled. The PI gain is not decreased when active damping is enabled, as proposed in Section VI, in order to avoid the resonance being damped due to the smaller PI gain.

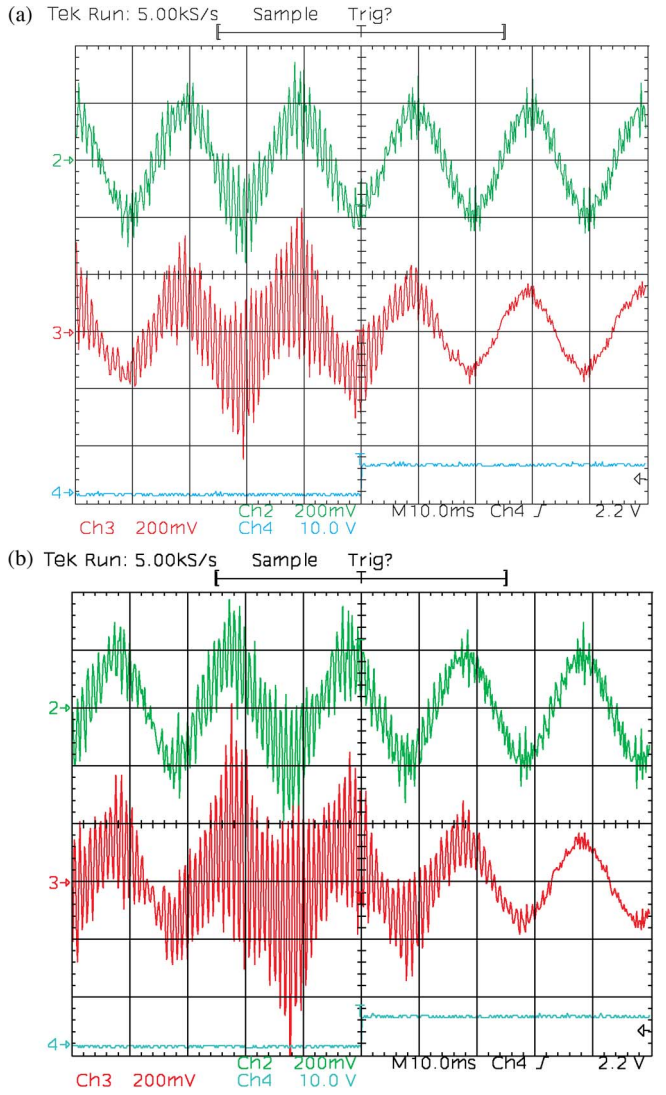

Fig. 5. Effect of active damping with (a) notch filter and (b) low-pass filter for high relative resonance frequency $f_{\mathrm{Res}} = 0.62 \cdot f_C/2$. Converter phase current (Ch. 2: 20 A/div), line phase current (Ch. 3: 20 A/div) and enabled signal of active damping filtering (low: off; high: on).

Figs. 5 and 6 show the effect of active damping filtering for high and low relative resonance frequencies, respectively. For the high relative resonance frequency, both the low-pass and notch filters yield good resonance damping, as predicted in Tables IV and VI, respectively. For the low relative resonance frequency, only notch filtering can stabilize the system. The low-pass filtering yields instability, as can be clearly seen from Fig. 6(b). The current oscillations are considerably increased until the converter finally trips. Note that, for better visualization, the result with low-pass filters in Fig. 6(b) is obtained with a slightly reduced PI gain. In this case, the system without active damping is close to the stability limit, but no huge oscillations appear unless active damping is activated.

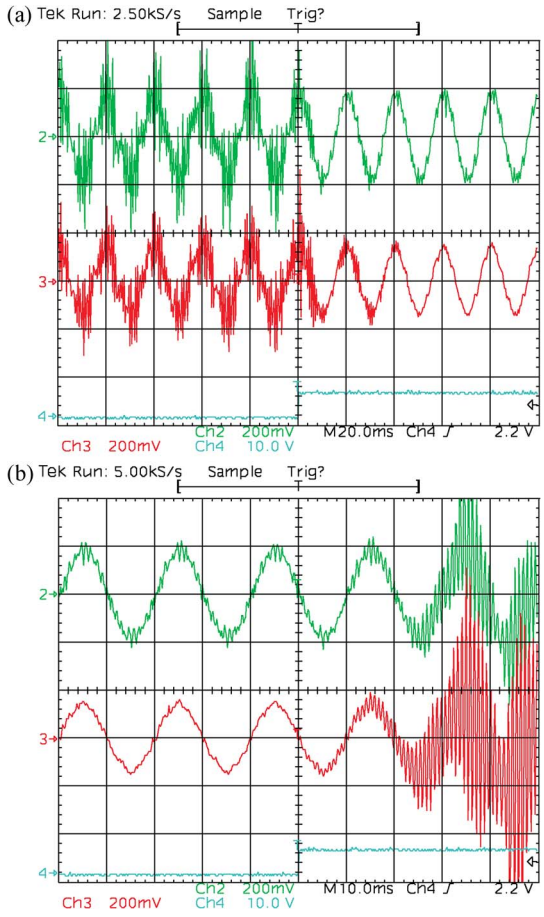

Fig. 6. Effect of active damping with (a) notch filter and (b) low-pass filter for low relative resonance frequency $f_{\mathrm{Res}} = 0.31 \cdot f_C/2$. Converter phase current (Ch. 2: 20 A/div), line phase current (Ch. 3: 20 A/div) and enabled signal of active damping filtering (low: off; high: on).

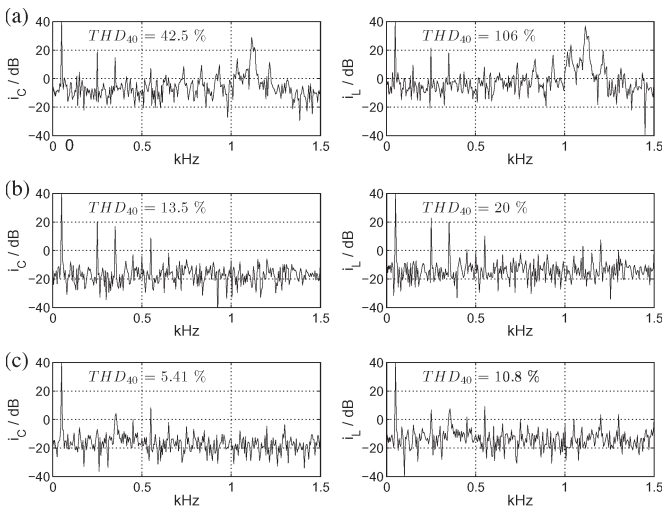

Fig. 7. Steady-state frequency content and THD of the (left) measured phase converter current and (right) line current. (a) Without active damping filter. (b) With notch filter. (c) With notch filter and resonant controller for compensation of the sixth harmonic in the dq-frame.

In Fig. 7, the frequency content of the currents is shown for various controller settings. When only PI controllers are used, the resonance is clearly excited at 1.23 kHz [see Fig. 7(a)]. Moreover, some low-frequency distortions caused by background grid voltage harmonics are visible. Even though the resonance gets well damped by active damping filtering, the low frequency distortions slightly increase as the controller bandwidth suffers from filtering [see Fig. 7(b)]. It is common practice to apply harmonic compensators for at least the fifth and seventh harmonic frequencies [1]. By that, the harmonic distortion gets reduced to an acceptable level [see Fig. 7(c)]. The total harmonic distortion (THD) factor, as defined in (8) in the Appendix, also indicates the improvements.

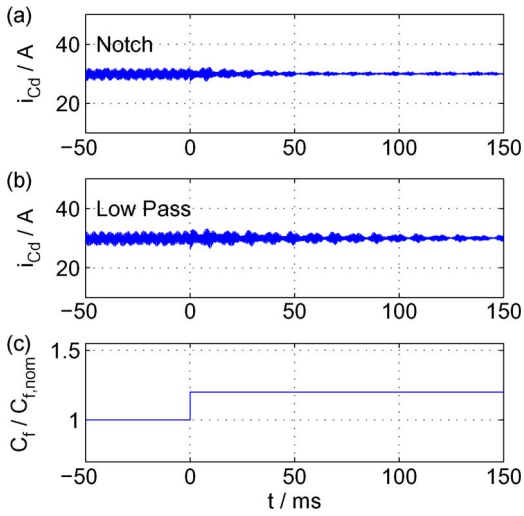

Fig. 8. Robustness test with a 20% step of filter capacitance C_f. (a) Notch-filter response. (b) Low-pass-filter response. (c) Actual filter capacitance value.

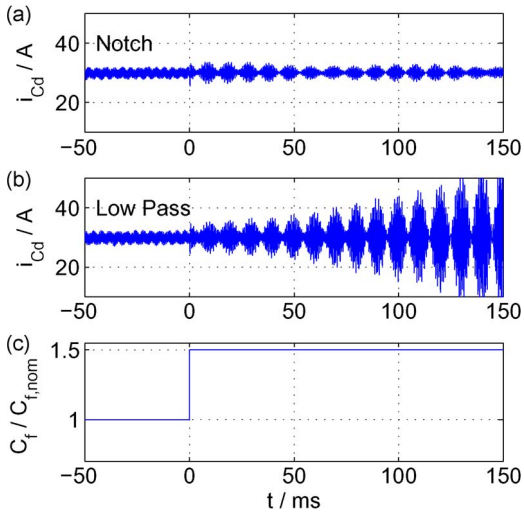

Fig. 9. Robustness test with a 50% step of filter capacitance C_f. (a) Notch-filter response. (b) Low-pass-filter response. (c) Actual filter capacitance value.

B. Test of Robustness of Active Damping (Simulation)

For the testing of the robustness, the filter capacitance C_f is changed within one control period. In Fig. 8, the capacitance is increased from 100% to 120% of the nominal capacitance. The effective resonance frequency is reduced to 91%. Both the notch and low-pass filters stay stable after a short transient. Fig. 9 shows the response to a step from 100% to 150% of the nominal capacitance. It can be seen that the notch filter is robust

TABLE VIII
ACTIVE DAMPING FILTER PARAMETERS

	Low pass filter	Lead-Element	Notch filter	Bi-quad filter
Continuous transfer function G(s)	$\frac{\omega_f^2}{s^2+2D\omega_f s+\omega_f^2}$	$\frac{s/\omega_f+1}{s\alpha/\omega_f+1}$	$\frac{s^2+2D_z\omega_f s+\omega_f^2}{s^2+2D_p\omega_f s+\omega_f^2}$	$\frac{s^2+2D_z\omega_z s+\omega_z^2}{s^2+2D_p\omega_p s+\omega_p^2}$
Parameters of discrete transfer function G(z), see (3)				
a_2	ω_f^2	0	$(c_D^2+2D_z c_D\omega_f+\omega_f^2)$	$(c_D^2+2D_z c_D\omega_f+\omega_z^2)$
a_1	$2\omega_f^2$	$\frac{c_D}{\omega_f}+1$	$-(2c_D^2-2\omega_f^2)$	$-(2c_D^2-2\omega_z^2)$
a_0	ω_f^2	$1-\frac{c_D}{\omega_f}$	$(c_D^2-2D_z c_D\omega_f+\omega_f^2)$	$(c_D^2-2D_z c_D\omega_z+\omega_z^2)$
b_2	$(c_D^2+2Dc_D\omega_f+\omega_f^2)$	0	$(c_D^2+2D_p c_D\omega_f+\omega_f^2)$	$(c_D^2+2D_p c_D\omega_p+\omega_p^2)$
b_1	$-(2c_D^2-2\omega_f^2)$	$\frac{c_D\alpha}{\omega_f}+1$	$-(2c_D^2-2\omega_f^2)$	$-(2c_D^2-2\omega_p^2)$
b_0	$(c_D^2-2Dc_D\omega_f+\omega_f^2)$	$1-\frac{c_D\alpha}{\omega_f}$	$(c_D^2-2D_p c_D\omega_f+\omega_f^2)$	$(c_D^2-2D_p c_D\omega_p+\omega_p^2)$
Discretization coefficient c_D (Tustin with Prewarping)	$\omega_f/tan(\omega_f T_c/2)$			

enough, whereas the low-pass filters cannot keep the resonance damped as its frequency reduces too much.

IX. CONCLUSION

Filter-based approaches for solving specific control problems of grid-connected PWM converters with respect to harmonic rejection are a well-established procedure both in current control and synchronization. The easy plug-in feature and the physical meaning are the two main advantages of this approach, which is straightforward also for enhancing the stability of the converter when an LCL filter is used on the grid side. In this case, the filter part of the controller serves for damping the potentially unstable dynamics of the LCL filter. The resulting active damping solution is attractive also because the alternative is to use more complex control structures that need more sensors or complex estimators. This paper has offered a systematic study of the filter-based active damping with reference to the bandwidth, robustness, and complexity. Different approaches are compared, highlighting their performance and limitations in case of different positions of the current sensors and different resonance frequencies. The tuning procedures are discussed, and the impact on low- and high-frequency harmonic contents is investigated through simulations and experimental results. The notch-filter solution is proven to be the most flexible and effective active damping method even if it is not needed in all the possible depicted scenarios. In fact, the low-pass filter can be enough in case of line-current feedback and a medium–low resonance frequency that is frequently found in medium-power distributed generation systems.

APPENDIX

a) Filter Transfer Functions: The discretization of the continuous filter functions shown in Table VIII is done with Tustin approximation with prewarping around the filter frequency ω_f [50]. In fact, the effectiveness of the active damping by the notch filters is deeply affected by the method of discretization [50], [51]. The parameters of the discrete transfer function of (3) are listed in Table VIII.

For the notch filter, the following relations between the damping coefficients D_z and D_p can be derived from the $G(s)$ of Table VIII in terms of ω_f, $\Delta\omega_f$, $a_{\omega f}$, and a_Δ:

$$D_p = \left|\frac{2\omega_f\Delta\omega_f+\Delta\omega_f^2}{2\omega_f\Delta\omega_f+\omega_f^2}\right|\sqrt{\frac{1-a_\Delta^2}{a_\Delta^2-a_{\omega f}^2}} \tag{6}$$

$$D_z = a_{\omega f}D_p a_{\omega f} < a_\Delta. \tag{7}$$

The notch-filter parameters D_p and D_z are initially obtained from (6). As the attenuation of the discrete filter varies slightly from the continuous one at the border of the specified frequency band, they are slightly adjusted in order to obtain a_Δ at $\omega_f \pm \Delta\omega_f$.

b) THD: The THD is defined as

$$\text{THD}_{40} = \sqrt{\sum_{h=2}^{40}\left(\frac{\tilde{I}_h}{\tilde{I}_1}\right)^2}. \tag{8}$$

REFERENCES

[1] F. Blaabjerg, R. Teodorescu, M. Liserre, and A. Timbus, "Overview of control and grid synchronization for distributed power generation systems," *IEEE Trans. Ind. Electron.*, vol. 53, no. 5, pp. 1398–1409, Oct. 2006.

[2] M. Liserre, T. Sauter, and J. Hung, "Integrating renewable energy sources into the smart power grid through industrial electronics," *IEEE Ind. Electron. Mag.*, vol. 4, no. 1, pp. 18–37, Mar. 2010.

[3] R. Teodorescu, M. Liserre, and R. Rodriguez, *Grid Converters for Photovoltaic and Wind Power Systems*. Hoboken, NJ: Wiley, 2010.

[4] M. Liserre, F. Blaabjerg, and S. Hansen, "Design and control of an LCL-filter-based three-phase active rectifier," *IEEE Trans. Ind. Appl.*, vol. 41, no. 5, pp. 1281–1291, Sep./Oct. 2005.

[5] R. Teichmann, M. Malinowski, and S. Bernet, "Evaluation of three-level rectifiers for low-voltage utility applications," *IEEE Trans. Ind. Electron.*, vol. 52, no. 2, pp. 471–481, Apr. 2005.

[6] P. Channegowda and V. John, "Filter optimization for grid interactive voltage source inverters," *IEEE Trans. Ind. Electron.*, vol. 57, no. 12, pp. 4106–4114, Dec. 2010.

[7] F. Blaabjerg, E. Chiarantoni, A. Dell'Aquila, M. Liserre, and S. Vegura, "Sensitivity analysis of a LCL-filter based three-phase active rectifier via a 'virtual circuit' approach," *J. Circuits, Syst., Comput.—Jubilee Special Issue on Power Electronics*, vol. 13, no. 4, pp. 665–686, Aug. 2004.

[8] G. Shen, D. Xu, L. Cao, and X. Zhu, "An improved control strategy for grid-connected voltage source inverters with an LCL filter," *IEEE Trans. Power Electron.*, vol. 23, no. 4, pp. 1899–1906, Jul. 2008.

[9] C. Olalla, R. Leyva, A. El Aroudi, and I. Queinnec, "Robust LQR control for PWM converters: An LMI approach," *IEEE Trans. Ind. Electron.*, vol. 56, no. 7, pp. 2548–2558, Jul. 2009.

[10] T. Wang, Z. Ye, G. Sinha, and X. Yuan, "Output filter design for a grid-interconnected three-phase inverter," in *Proc. IEEE 34th Annu. Power Electron. Spec. Conf.*, Jun. 2003, vol. 2, pp. 779–784.

[11] V. Blasko and V. Kaura, "A novel control to actively damp resonance in input LC filter of a three-phase voltage source converter," *IEEE Trans. Ind. Appl.*, vol. 33, no. 2, pp. 542–550, Mar./Apr. 1997.
[12] M. Liserre, A. Dell'Aquila, and F. Blaabjerg, "Stability improvements of an LCL-filter based three-phase active rectifier," in *Proc. 33rd IEEE Annu. Power Electron. Spec. Conf.*, 2002, vol. 3, pp. 1195–1201.
[13] A. Rahimi and A. Emadi, "Active damping in dc/dc power electronic converters: A novel method to overcome the problems of constant power loads," *IEEE Trans. Ind. Electron.*, vol. 56, no. 5, pp. 1428–1439, May 2009.
[14] M. Liserre, R. Teodorescu, and F. Blaabjerg, "Stability of photovoltaic and wind turbine grid-connected inverters for a large set of grid impedance values," *IEEE Trans. Power Electron.*, vol. 21, no. 1, pp. 263–272, Jan. 2006.
[15] I. J. Gabe, V. F. Montagner, and H. Pinheiro, "Design and implementation of a robust current controller for VSI connected to the grid through an LCL filter," *IEEE Trans. Power Electron.*, vol. 24, no. 6, pp. 1444–1452, Jun. 2009.
[16] E. Twining and D. Holmes, "Grid current regulation of a three-phase voltage source inverter with an LCL input filter," *IEEE Trans. Power Electron.*, vol. 18, no. 3, pp. 888–895, May 2003.
[17] P. Loh and D. Holmes, "Analysis of multiloop control strategies for $LC/CL/LCL$-filtered voltage-source and current-source inverters," *IEEE Trans. Ind. Appl.*, vol. 41, no. 2, pp. 644–654, Mar./Apr. 2005.
[18] M. Bierhoff and F. Fuchs, "Active damping for three-phase PWM rectifiers with high-order line-side filters," *IEEE Trans. Ind. Electron.*, vol. 56, no. 2, pp. 371–379, Feb. 2009.
[19] J. Dannehl, F. Fuchs, S. Hansen, and P. Thgersen, "Investigation of active damping approaches for PI-based current control of grid-connected pulse width modulation converters with LCL filters," *IEEE Trans. Ind. Appl.*, vol. 46, no. 4, pp. 1509–1517, Jul./Aug. 2010.
[20] W. Zhao, Y. Li, and G. Chen, "A double-loop current control strategy for shunt active power filter with LCL filter," in *Proc. IEEE ISIE*, Jul. 2009, pp. 1841–1845.
[21] Y. W. Li, "Control and resonance damping of voltage-source and current-source converters with LC filters," *IEEE Trans. Ind. Electron.*, vol. 56, no. 5, pp. 1511–1521, May 2009.
[22] Q. Zhang, L. Qian, C. Zhang, and D. Cartes, "Study on grid connected inverter used in high power wind generation system," in *Conf. Rec. 41st IEEE IAS Annu. Meeting*, Oct. 2006, vol. 2, pp. 1053–1058.
[23] F. Magueed and J. Svensson, "Control of VSC connected to the grid through LCL-filter to achieve balanced currents," in *Conf. Rec. IEEE IAS Annu. Meeting*, 2005, vol. 1, pp. 572–578.
[24] L. Serpa, S. Ponnaluri, P. Barbosa, and J. Kolar, "A modified direct power control strategy allowing the connection of three-phase inverters to the grid through LCL filters," *IEEE Trans. Ind. Appl.*, vol. 43, no. 5, pp. 1388–1400, Sep./Oct. 2007.
[25] W. Gullvik, L. Norum, and R. Nilsen, "Active damping of resonance oscillations in LCL-filters based on virtual flux and virtual resistor," in *Proc. Eur. Conf. Power Electron. Appl.*, Sep. 2007, pp. 1–10.
[26] M. Malinowski and S. Bernet, "A simple voltage sensorless active damping scheme for three-phase PWM converters with an LCL filter," *IEEE Trans. Ind. Electron.*, vol. 55, no. 4, pp. 1876–1880, Apr. 2008.
[27] J. Vasquez, J. Guerrero, A. Luna, P. Rodriguez, and R. Teodorescu, "Adaptive droop control applied to voltage-source inverters operating in grid-connected and islanded modes," *IEEE Trans. Ind. Electron.*, vol. 56, no. 10, pp. 4088–4096, Oct. 2009.
[28] A. Draou, Y. Sato, and T. Kataoka, "A new state feedback based transient control of PWM ac to dc voltage type converters," *IEEE Trans. Power Electron.*, vol. 10, no. 6, pp. 716–724, Nov. 1995.
[29] E. Wu and P. Lehn, "Digital current control of a voltage source converter with active damping of LCL resonance," *IEEE Trans. Power Electron.*, vol. 21, no. 5, pp. 1364–1373, Sep. 2006.
[30] F. Liu, Y. Zhou, S. Duan, J. Yin, and B. Liu, "Parameter design of a two-current-loop controller used in a grid-connected inverter system with LCL filter," *IEEE Trans. Ind. Electron.*, vol. 56, no. 11, pp. 4483–4491, Nov. 2009.
[31] M. Bongiorno and J. Svensson, "Voltage dip mitigation using shunt-connected voltage source converter," *IEEE Trans. Power Electron.*, vol. 22, no. 5, pp. 1867–1874, Sep. 2007.
[32] P.-T. Cheng, J.-M. Chen, and C.-L. Ni, "Design of a state-feedback controller for series voltage-sag compensators," *IEEE Trans. Ind. Appl.*, vol. 45, no. 1, pp. 260–267, Jan./Feb. 2009.
[33] J. Dannehl, F. Fuchs, and P. Thgersen, "PI state space current control of grid-connected PWM converters with LCL filters," *IEEE Trans. Power Electron.*, vol. 25, no. 9, pp. 2320–2330, Sep. 2010.
[34] B. Bolsens, K. De Brabandere, J. Van den Keybus, J. Driesen, and R. Belmans, "Model-based generation of low distortion currents in grid-coupled PWM-inverters using an LCL output filter," *IEEE Trans. Power Electron.*, vol. 21, no. 4, pp. 1032–1040, Jul. 2006.
[35] F. Huerta, E. Bueno, S. Cobreces, F. Rodriguez, and C. Giron, "Control of grid-connected voltage source converters with LCL filter using a linear quadratic servocontroller with state estimator," in *Proc. IEEE Power Electron. Spec. Conf.*, Jun. 2008, pp. 3794–3800.
[36] S. Mariethoz and M. Morari, "Explicit model-predictive control of a PWM inverter with an LCL filter," *IEEE Trans. Ind. Electron.*, vol. 56, no. 2, pp. 389–399, Feb. 2009.
[37] K. H. Ahmed, A. M. Massoud, S. J. Finney, and B. W. Williams, "A modified stationary reference frame-based predictive current control with zero steady-state error for LCL coupled inverter-based distributed generation systems," *IEEE Trans. Ind. Electron.*, vol. 58, no. 4, pp. 1359–1370, Apr. 2011.
[38] K. Acharya, S. Mazumder, and I. Basu, "Reaching criterion of a three-phase voltage-source inverter operating with passive and nonlinear loads and its impact on global stability," *IEEE Trans. Ind. Electron.*, vol. 55, no. 4, pp. 1795–1812, Apr. 2008.
[39] A. Gensior, H. Sira-Ramirez, J. Rudolph, and H. Guldner, "On some nonlinear current controllers for three-phase boost rectifiers," *IEEE Trans. Ind. Electron.*, vol. 56, no. 2, pp. 360–370, Feb. 2009.
[40] L. Harnefors, L. Zhang, and M. Bongiorno, "Frequency-domain passivity-based current controller design," *IET Power Electron.*, vol. 1, no. 4, pp. 455–465, Dec. 2008.
[41] M. Liserre, A. Dell'Aquila, and F. Blaabjerg, "Genetic algorithm-based design of the active damping for an LCL-filter three-phase active rectifier," *IEEE Trans. Power Electron.*, vol. 19, no. 1, pp. 76–86, Jan. 2004.
[42] C. Dick, S. Richter, M. Rosekeit, J. Rolink, and R. De Doncker, "Active damping of LCL resonance with minimum sensor effort by means of a digital infinite impulse response filter," in *Proc. Eur. Conf. Power Electron. Appl.*, Sep. 2007, pp. 1–8.
[43] K.-S. Tang, K.-F. Man, S. Kwong, and Z.-F. Liu, "Design and optimization of IIR filter structure using hierarchical genetic algorithms," *IEEE Trans. Ind. Electron.*, vol. 45, no. 3, pp. 481–487, Jun. 1998.
[44] W.-T. Franke, J. Dannehl, F. W. Fuchs, and M. Liserre, "Characterization of differential-mode filter for grid-side converters," in *Proc. 35th IEEE IECON*, Nov. 2009, pp. 4080–4085.
[45] H. Unbehauen, *Regelungstechnik I,* 12th ed. Braunschweig, Germany: Vieweg-Verlag, 2002.
[46] W. S. Levine, *The Control Handbook*. Boca Raton, FL: CRC, 1995.
[47] J. Dannehl, C. Wessels, and F. Fuchs, "Limitations of voltage-oriented PI current control of grid-connected PWM rectifiers with LCL filters," *IEEE Trans. Ind. Electron.*, vol. 56, no. 2, pp. 380–388, Feb. 2009.
[48] M. Liserre, F. Blaabjerg, and R. Teodorescu, "Grid impedance estimation via excitation of LCL-filter resonance," *IEEE Trans. Ind. Appl.*, vol. 43, no. 5, pp. 1401–1407, Sep./Oct. 2007.
[49] J. Dannehl, F. Fuchs, and S. Hansen, "PWM rectifier with LCL-filter using different current control structures," in *Proc. Eur. Conf. Power Electron. Appl.*, Sep. 2007, pp. 1–10.
[50] A. Yepes, F. Freijedo, J. Doval-Gandoy, O. Lopez, J. Malvar, and P. Fernandez-Comesana, "On the discrete-time implementation of resonant controllers for active power filters," in *Proc. IEEE 35th IECON*, Nov. 2009, pp. 3686–3691.
[51] L. Harnefors, "Implementation of resonant controllers and filters in fixed-point arithmetic," *IEEE Trans. Ind. Electron.*, vol. 56, no. 4, pp. 1273–1281, Apr. 2009.

Joerg Dannehl (S'06–M'10) was born in Flensburg, Germany, in 1980. He received the Dipl.-Ing. degree from the Christian-Albrechts-University of Kiel, Kiel, Germany, in 2005.

In 2005, he was with the Institute for Power Electronics and Electrical Drives, Christian-Albrechts-University of Kiel, as a Research Assistant. Since August 2010, he has been with Danfoss Solar Inverters A/S, Sønderborg, Denmark, as a Control Engineer working in Product Development. His main research interests include the control of power converters and drives.

Mr. Dannehl is member of the IEEE Industrial Electronics Society, IEEE Power Electronics Society, and Verband der Elektrotechnik Elektronik Informationstechnik.

Marco Liserre (S'00–M'02–SM'07) received the M.Sc. and Ph.D. degrees in electrical engineering from the Bari Polytechnic, Bari, Italy, in 1998 and 2002, respectively.

Since January 2004, he has been with Bari Polytechnic, as an Assistant Professor teaching the courses of power electronics, industrial electronics, and electrical machines. He has been a Visiting Professor at the Aalborg University, Aalborg, Denmark, the Alcala de Henares University, Alcala de Henares, Spain, and the Christian-Albrechts-University of Kiel, Kiel, Germany. He has published 130 technical papers, 31 of them in international peer-reviewed journals, and three chapters of a book. These works have received more than 1500 citations.

Dr. Liserre is an Associate Editor of the IEEE TRANSACTIONS ON INDUSTRIAL ELECTRONICS. He is the Founder and was the Editor-in-Chief of the *IEEE Industrial Electronics Magazine* (2007–2009). He is the Founder and the Chairman of the Technical Committee on Renewable Energy Systems of the IEEE Industrial Electronics Society (IES). He is an Associate Editor of the IEEE TRANSACTIONS ON SUSTAINABLE ENERGY. He was a Cochairman of the *International Symposium on Industrial Electronics* (2010). He is the Vice President responsible of the publications of the IEEE IES. He was the recipient of the IES 2009 Early Career Award.

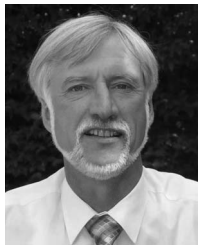

Friedrich Wilhelm Fuchs (M'96–SM'01) received the Dipl.-Ing. and Ph.D. degrees from the Rheinisch-Westfälische Technische Hochschule Aachen (RWTH) University of Technology Aachen, Aachen, Germany, in 1975 and 1982, respectively.

Since 1975, he carried out research work at the RWTH University of Technology Aachen on ac automotive drives. Between 1982 and 1991, he was a Group Manager of the development of power electronics and electrical drives in a medium-sized company. In 1991, he was with Allgemeine Elektrizitäts Gesellschaft (AEG), Berlin, Germany, where he was a Managing Director for the research, design, and development of drive products, drive systems, and high-power supplies, covering the power range from 5 kVA to 50 MVA, in the Converter and Drives Division, currently named as the Converteam. Since 1996, he has been with the Christian-Albrechts-University of Kiel, Kiel, Germany, as a full Professor and the Head of the Institute for Power Electronics and Electrical Drives, which he and his team built up. His institute is a member of CEwind e.G., a registered corporative competence center of research for the universities in wind energy Schleswig-Holstein, as well as of Kompetenzzentrum Leistungselektronik Schleswig-Holstein (KLSH), the competence center for power electronics in Schleswig-Holstein, where combined research projects are carried out. He has authored or coauthored more than 140 papers. His research work has been on power semiconductor application, converter topologies, and variable speed drives as well as on their control, which is documented in many publications. There is a special focus on renewable energy conversion, particularly on wind and solar energy, on the nonlinear control of drives, and on automotive drives as well as on the diagnosis of drives and fault-tolerant drives. He has established a wind-power converter generator laboratory, where many research projects are carried out with industrial partners.

Dr. Fuchs is the Chairman of the supervisory board of Cewind e.G., a Convenor of [Deutsche Kommission Elektrotechnik (DKE), International Electrotechnical Commission (IEC)], and an International Speaker for the standardization of power electronics as well as a member of Verband der Elektrotechnik Elektronik Informationstechnik (VDE) and European Power Electronics And Drives Association (EPE).